Fast linearized coronagraph optimizer (FALCO) III: optimization of key coronagraph design parameters

Carl T. Coker, Garreth Ruane, A J Eldorado Riggs, Erkin Sidick, Byoung-Joon Seo, et al.

Carl T. Coker, Garreth Ruane, A J Eldorado Riggs, Erkin Sidick, Byoung-Joon Seo, Brian Kern, David Marx, Stuart Shaklan, "Fast linearized coronagraph optimizer (FALCO) III: optimization of key coronagraph design parameters," Proc. SPIE 10698, Space Telescopes and Instrumentation 2018: Optical, Infrared, and Millimeter Wave, 1069851 (7 August 2018); doi: 10.1117/12.2313788

SPIE.

Event: SPIE Astronomical Telescopes + Instrumentation, 2018, Austin, Texas, United States

Fast Linearized Coronagraph Optimizer (FALCO) III. Optimization of key coronagraph design parameters

Carl T. Coker[a,b], Garreth Ruane[c], A J Eldorado Riggs[b], Erkin Sidick[b], Byoung-Joon Seo[b], Brian Kern[b], David Marx[b], and Stuart Shaklan[b]

[a]NASA Postdoctoral Program Fellow
[b]Jet Propulsion Laboratory, California Institute of Technology, 4800 Oak Grove Drive, Pasadena, CA 91109
[c]California Institute of Technology, 1200 E California Blvd, Pasadena, CA 91125

ABSTRACT

Deformable mirrors (DMs) are increasingly becoming part of nominal coronagraph designs, such as the hybrid Lyot coronagraph, in addition to their role counteracting optical aberrations. Previous studies have investigated the effects of the inter-DM Fresnel number on achievable contrast, throughput, and tip/tilt sensitivity for apodized coronagraphs augmented with DMs to suppress diffraction from struts and segment gaps. In this paper, we build upon that previous work by directly suppressing tip/tilt sensitivity with the controller, both for coronagraphs with and without apodizers. We also explore the effects of other important design parameters such as actuator density and tip/tilt controller weighting on performance. These comprehensive coronagraph design studies are enabled by the Fast Linearized Coronagraph Optimizer (FALCO) software toolbox, which provides rapid re-calculation of the DM response matrix for a variety of coronagraphs.

Keywords:

1. INTRODUCTION

Imaging and characterizing exoplanets in reflected light is one of the foremost technical challenges in astronomy today. Great strides have been made in coronagraph technology over the past two decades, with the goal of using a coronagraph with future telescopes such as the Wide-Field Infrared Survey Telescope (WFIRST),[1] the Large Ultraviolet Infrared Telescope (LUVOIR)[2] and Habitable Exoplanet Imaging Mission (HabEx)[3] concepts, the European Extremely Large Telescope (ELT),[4,5] and the Thirty Meter Telescope (TMT).[6] Earth-like exoplanets in particular represent a very difficult problem, with the coronagraph needing to achieve $\sim 10^{-10}$ contrast or better in visible light.

One of the largest limitations on present coronagraph design efforts is the computational complexity of the problem, resulting in long calculation times of hours or days per coronagraphic system, making large surveys of the design parameter space prohibitive. The difficulty is only enhanced by the possibility of using deformable mirrors (DMs) for performing diffraction control of telescope struts, segment gaps, and other pupil obscurations. The Fast Linearized Coronagraph Optimizer (FALCO; see FALCO I in these proceedings)[7] represents a dramatic speed-up over previous wavefront control codes,[8] making surveys of DM-enhanced coronagraphs feasible, particularly for future telescopes equipped with extremely high DM actuator densities.

Since DMs may be able to be used to completely compensate for the non-axisymmetric portions of the telescope pupil, it may be feasible to use 1D-optimized coronagraph masks instead of the typical 2D-optimized ones. This would be a tremendous time-saver, as 1D coronagraph masks can be computed very quickly for a given set of instrument parameters, allowing large surveys for optimal science yield to be performed using ordinary computer hardware in just a few days. In this paper, we conduct a trade study for a deformable mirror shaped pupil Lyot coronagraph (DMSPLC) for the LUVOIR Architecture A (hereafter referred to just as LUVOIR A) aperture.[2] We begin by optimizing a 1D-radial shaped pupil mask, and then use FALCO to study the effects of

Further author information: (Send correspondence to Carl T. Coker)
Carl T. Coker: E-mail: carl.t.coker@jpl.nasa.gov, Telephone: 1 818 354 0104

Space Telescopes and Instrumentation 2018: Optical, Infrared, and Millimeter Wave, edited by Makenzie Lystrup, Howard A. MacEwen, Giovanni G. Fazio, Proc. of SPIE Vol. 10698, 1069851
 · doi: 10.1117/12.2313788

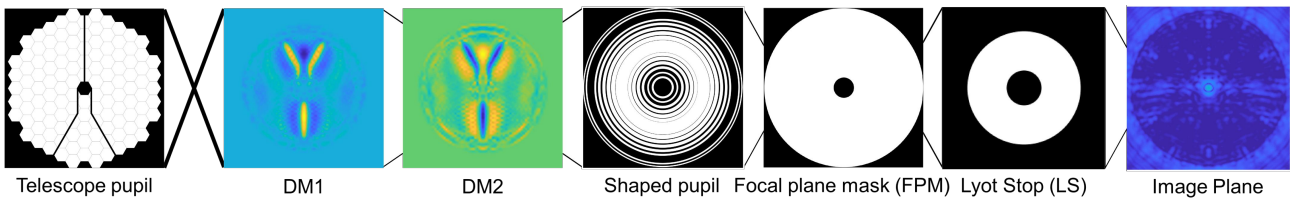

Figure 1. Schematic of the optical path for the coronagraph under study in this paper. We use the LUVOIR A telescope aperture followed by two DMs, one in a pupil plane and another a specified distance away from the first. The light then goes to a binary-amplitude circularly symmetric shaped pupil mask and is focused onto a focal plane mask designed to block the on-axis star. The light then goes through a Lyot stop before being focused to produce the final image.

changing the inter-DM Fresnel number, the number of actuators across the DM, and adding a finite-sized star. In so doing, we seek to determine the feasibility of the DMSPLC for future large segmented telescopes such as the LUVOIR concept.

In Section 2, we describe our 1D coronagraph optimization code. In Section 3, we describe our shaped pupil Lyot coronagraph survey using the 1D code and present its results. In Section 4, we describe our 2D survey of DM parameters and its results, and in Section 5 we provide a brief discussion and conclusion.

2. 1D SPLC OPTIMIZATION CODE

In the past decade, 1D coronagraph optimizations have fallen out of favor because 1D coronagraph designs cannot correct for non-axisymmetric pupil features such as struts and segment gaps. However, DMs can control the diffraction from those features,[9] perhaps making 1D-optimized coronagraph masks usable. 1D-optimized pupil masks have two main advantages over 2D-optimized ones: first, they can be computed much more quickly, making large searches of parameter space feasible; and second, several key coronagraph performance metrics (throughput, contrast, and inner working angle; IWA) improve with a 1D-radial apodizer over one including struts and segment gaps. Using a binary shaped pupil mask as opposed to a grayscale apodizer saves a step in having to convert a grayscale pattern to binary microdots.

We have written a 1D-radial SPLC optimization code, which we plan to release in the near future as part of the 1D-Radial Optimization Suite (1DROS) software toolbox for 1D optimization and modeling of coronagraphs. Our 1D SPLC code first prepares the Jacobian/optical propagation matrix for a given set of focal plane mask and Lyot stop parameters and a given set of wavelengths, then feeds this along with a set of contrast constraints into CVXPY,[10,11] a freely available convex optimization suite written in Python. We optimized for maximum throughput, resulting in binary-amplitude masks. To complete the survey, we simply derived a mask for each set of parameters we wish to investigate, producing a mask for every point in the parameter space. Each mask takes only a few seconds to compute, and the survey is embarrassingly parallelizable, as no mask depends on results from another. The survey described in this work was performed in approximately six hours using eight nodes of the Aurora supercomputing cluster at the Jet Propulsion Laboratory (JPL).

3. 1D SPLC SURVEY

3.1 1D Survey Parameters

The goal of our design survey was to find the shaped pupil mask which produced the maximum planet yield for a 1D version of the LUVOIR A pupil (the telescope pupil in Figure 1) with no struts or segment gaps. The design contrast goal was $10^{-10.5}$ to provide a slight buffer for the expected drop in performance when compensating for the segment gaps and struts with DMs. We used a spectral bandwidth ($\Delta\lambda/\lambda_0$) of 10%, a central wavelength of 500 nm, and used six wavelengths for evaluation. We then surveyed over the focal plane mask's inner and outer radius and Lyot stop's inner and outer diameter. The survey parameter ranges are shown in Table 1. We used 500 radial samples in the pupil mask plane and 250 in the Lyot plane; these were chosen as the minimum to avoid numerical artifacts.

Table 1. 1D SPLC Survey Parameters

FPM inner radius	$3.2 - 3.7\,\lambda/D$
FPM outer radius	$24 - 28\,\lambda/D$
Lyot stop inner diameter	$0.15 - 0.3$
Lyot stop outer diameter	$0.76 - 0.85$

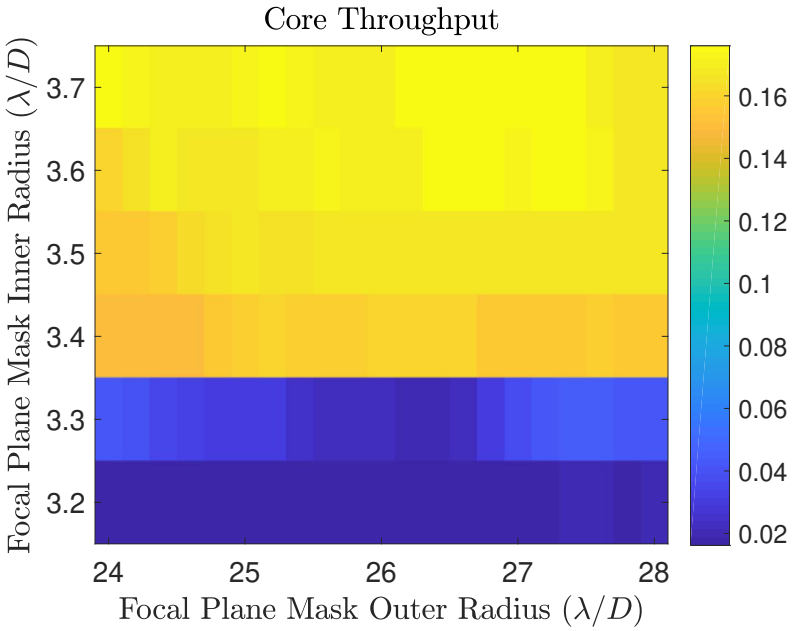

Figure 2. Core throughput as a function of focal plane mask inner and outer radius. The core throughput as defined in this paper is the ratio of the energy under the off-axis PSF core's main lobe that is above half-maximum to the total energy in the input pupil. As the FPM inner radius gets smaller, it becomes more difficult for the shaped pupil mask to maintain a given level of contrast over the dark hole, and it blocks more light, reducing throughput. Eventually, it becomes impossible for the mask to sufficiently control the light in the inner region of the dark hole, and the throughput craters, resulting in the cliff seen in the Figure. The highest exoplanet yield is found up against the cliff.

3.2 1D Survey Results

Figures 2 and 3 show the parameters of the highest throughput solutions for each focal plane mask. Assuming the telescope itself is fixed, inner working angle (IWA) is the most critical parameter for a coronagraph in terms of planet yield,[12] so the best mask is the one which offers the best IWA while still maintaining reasonable throughput. With SPLCs, this takes the form of a throughput "cliff" at a certain FPM inner radius, which effectively sets the IWA. This cliff is easily seen in Figure 2, showing up at $\sim 3.37\,\lambda/D$. As throughput is relatively stable with the choice of FPM outer radius, and thus outer working angle (OWA), the choice of OWA is instead set by the size of the region controllable by the DMs. For the 64x64-actuator DMs we simulated, this is $\sim 30\,\lambda/D$. Therefore, we chose a final mask with a $3.367\,\lambda/D$ FPM inner radius, $26.4\,\lambda/D$ FPM outer radius, $0.24D$ Lyot stop inner diameter, and $0.78D$ Lyot stop outer diameter. This is the same mask shown at the shaped pupil position in Figure 1.

4. 2D SPLC OPTIMIZATION USING FALCO

4.1 2D DMSPLC Survey

With the 1D-optimized shaped pupil mask in hand, we added two DMs to the optical path to correct for the struts and segment gaps in the simulated telescope pupil. We placed the first DM in a pupil plane and the second a given distance away from the first. Our 2D survey focused on the DMs, looking at three different parameters: the inter-DM Fresnel number (i.e., their separation), the number of actuators across the DM surface, and tip/tilt

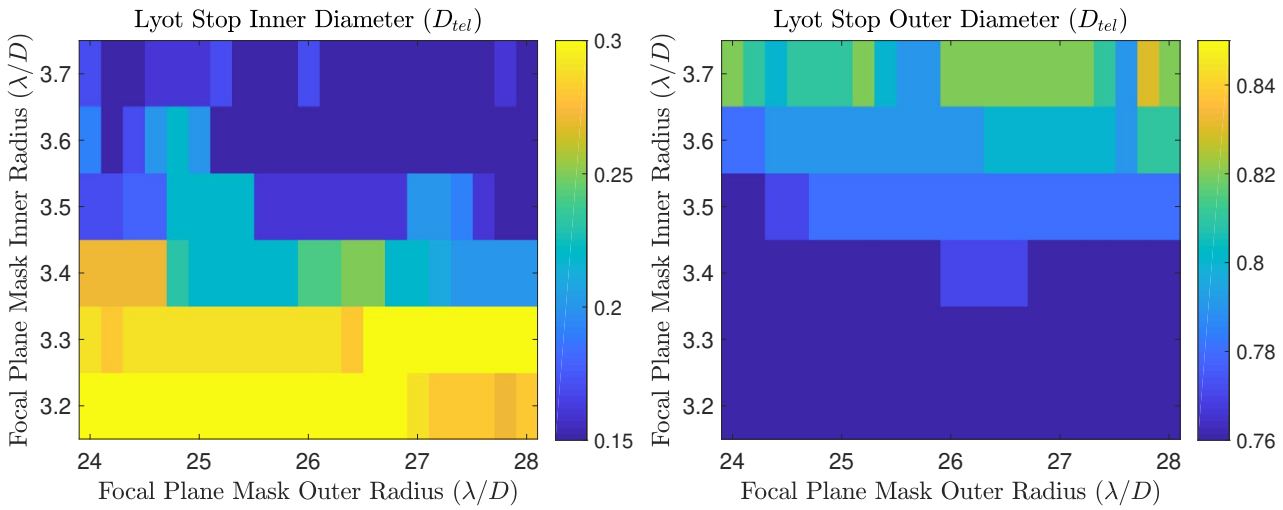

Figure 3. Lyot stop inner and outer diameter as a function of focal plane mask size. At the cliff, the Lyot stop suddenly becomes much more restrictive, cutting off an unacceptably large portion of the planet light.

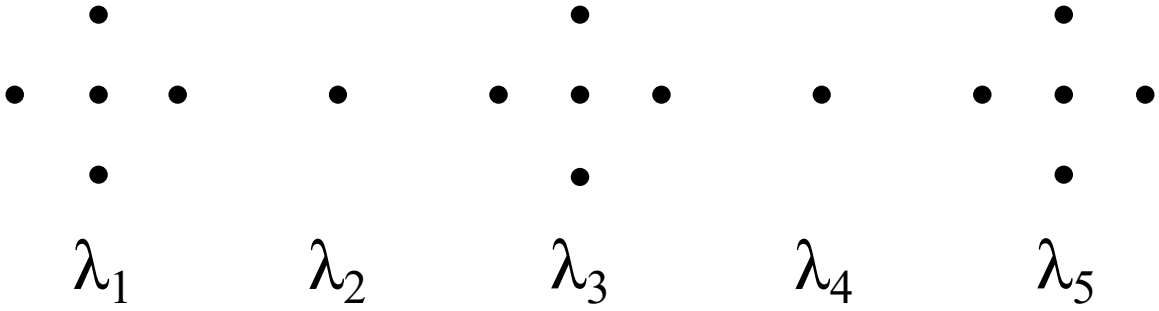

Figure 4. Diagram of our tip/tilt constellation at each control wavelength. We used 5 wavelengths to cover the 10% bandpass, but only controlled the outer tip/tilt offset points at three of them to save computation time without losing accuracy. The outer control points were offset from the center by 0.5 mas to give a stellar diameter of 1 mas.

control using the DMs. The first two parameters are pivotal for the design of the instrument, as they set the size of the beam inside the instrument and the physical scale. Large-diameter DMs require more space and propagation distance, so using the minimum number of actuators possible is desirable; smaller DMs are also less costly and more reliable. Tip/tilt sensitivity suppression is essential because stars have a nonzero angular size, causing light leakage that must be controlled somehow.

To conduct the survey, we used the Fast Linearized Coronagraph Optimizer (FALCO).[7] FALCO combines several propagation methods to efficiently model wavefront propagation through a coronagraph, resulting in a large speed increase over conventional brute-force optical propagation.[8] This allows us to thoroughly explore the parameter space in a reasonable amount of time - the final survey took approximately two weeks of computation time on a single workstation with 16 cores.

For the tip/tilt sensitivity control, we used five point sources to represent a star in a cross shape (Figure 4). We used 5 wavelengths across the 10% bandpass, only controlling the outer tip/tilt offset points at three of those wavelengths to save computation time. Evaluation of the 5-point solution using a disk model of a star showed the 5-point model to be sufficient. We offset the outer tip/tilt points by 0.5 mas from the central point, giving a stellar diameter of 1 mas ($0.15\lambda/D$ at 500 nm wavelength).

4.2 2D Survey Results

Figure 5 plots achieved average contrast in the dark hole vs. inter-DM Fresnel number for our best 1D mask and 64x64-actuator DMs. We used 20 EFC iterations to arrive at these points. The point source solutions are significantly better than those using a 1 mas diameter star, with the best performance coming at a Fresnel number of 576. The finite-sized star raises the contrast floor by a factor of ~ 4 in the best performance region (black points). Adding tip/tilt control (red points), that is, attempting to use the DMs to correct for the finite size of the star, provides only a small average benefit, most of which is concentrated at the outer correction radius, which is ultimately the least important part of the image for finding planets. Figure 6 shows the dark holes for each case (point source, finite-sized star and tip/tilt control, finite-sized star without tip/tilt control), while Figure 7 shows the ratio of the intensity of the dark holes for the finite-sized star with and without tip/tilt control enabled. Aside from the improvements shown at the outer correction radius, adding tip/tilt control mostly moves light around the dark hole rather than suppressing it.

These results imply that DMs on large aperture telescopes cannot simultaneously control well for a large stellar diameter and telescope struts/segment gaps. Typical stars of angular diameter $\sim 1\,\text{mas}$ represent a relatively large amount of tip/tilt ($0.15\,\lambda/D$ at 500 nm wavelength) on the $15\,m$ aperture tested here, so DMSPLCs may still be practical for smaller telescopes or smaller stars. The core throughput for each of the points in Figure 5 is shown in Figure 8. Only a $\sim 5\%$ relative throughput degradation is seen with the finite star. Interestingly, the throughput drop occurs whether or not tip/tilt control is explicitly enabled. We posit that this is simply a geometric effect of the stellar core smearing over a larger area.

We also examined the effect of the number of actuators on achievable contrast for point sources only. These data points are shown in Figure 9. The stairstep behavior seen in the simulations was unexpected, and we do not have a definitive explanation for it. We did expect to see increased contrast with increasingly large DMs as these mirrors offer more degrees of freedom for controlling the wavefront. Regardless of why the behavior occurs, 64x64-actuator DMs are sufficient to reach $\sim 10^{-10}$ contrast for our dark hole, obviating the need for larger DM concepts unless a larger outer working angle is desired.

5. CONCLUSIONS

In this paper, we conducted 1D and 2D trade studies for a DMSPLC for the LUVOIR A aperture. We used our 1D optimization code, 1DROS, to calculate a large variety of 1D shaped pupil masks based on a given set of focal plane mask and Lyot stop parameters. We then used the mask yielding the largest number of imageable exoplanets in FALCO, our 2D DM-optimization suite. Using FALCO, we investigated the effects of inter-DM Fresnel number, actuator count, and the finite size of the star on the performance of the coronagraph.

Our 1D survey was able to run quickly, producing $\sim 40,000$ shaped pupil masks in about six hours on a supercomputing cluster at JPL. This allowed us to thoroughly sample the parameter space and maximize expected planet yield for the dark hole size we could control with the DMs. 1D SPLCs display a "cliff" in throughput at some FPM inner radius where the throughput rapidly drops essentially to zero. Because planet yield is strongly dependent on IWA,[12] it is best to choose the system parameters corresponding to the precipice of the cliff. For our survey, that occurred at a FPM inner radius of $\sim 3.3\,\lambda/D$. The mask which resulted from that FPM and Lyot stop combination were fed into FALCO.

With FALCO, we studied the effect of inter-DM Fresnel number, number of actuators, and finite stellar size on the performance of a DMSPLC coronagraph for the LUVOIR A aperture. We found that there is a sweet spot for the separation between the DMs at an inter-DM Fresnel number of 576. Using this separation with 64x64-actuator DMs, which are already commercially available,[13] allows us to achieve $\sim 10^{-10}$ contrast averaged over the dark hole for an on-axis point source. This is also roughly where the best throughput is found. Interestingly, although the numerical value of our best inter-DM Fresnel number almost exactly matches a previous study,[14] they used a different definition of Fresnel number ($D^2/\lambda z$ vs. our $r^2/\lambda z$), meaning our results differ by a factor of 4. It is likely that differences in how the optical propagation is performed in each study are the reason behind the discrepancy.

We found that increasing the number of actuators across the DM results in better contrast in the dark hole. However, in our simulations it does so in an unusual way: instead of a smooth monotonically decreasing curve,

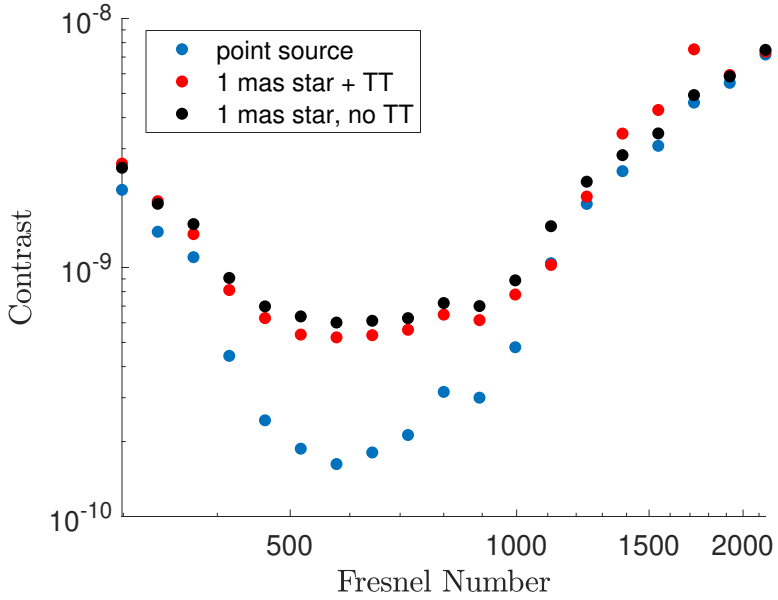

Figure 5. Contrast as a function of Fresnel number ($r^2/\lambda z$) for our 2D simulations using FALCO. All simulations shown use 64x64-actuator DMs, a 10% bandpass, and an outer working angle of $\sim 30\,\lambda/D$. The blue points used a point source star, the black points show a 1 mas diameter star with no tip/tilt control, and the red points show a 1 mas diameter star with tip/tilt control enabled. The DMs cannot simultaneously control for the struts, segment gaps, and the finite size of the star, as evidenced by the small difference between the having tip/tilt control enabled and not. Pupil apodization is likely required to reduce the sensitivity of the coronagraph to tip/tilt.

there is a stairstep behavior. Several times, contrast remains roughly flat with increasing actuator count until suddenly jumping down to a lower level. We do not know the exact cause of this behavior, but we suspect it is either related to the outer cutoff of the SPLC's FPM or some effect connected to a particular spatial frequency and its harmonics. Regardless, 64x64-actuator DMs are sufficient to achieve 10^{-10} contrast.

Adding a 1 mas diameter star dramatically reduced our achievable contrast, and attempting to use the DMs to control the extra tip/tilt failed to improve contrast to any significant degree. Rather, it appears that the DMs were mostly only able to move light around the dark hole instead of directing it outside the dark hole or to a blocked part of the field. This has serious implications for the viability of 1D-optimized coronagraphs augmented with DMs on obstructed large-aperture space telescopes such as the LUVOIR concept. Although they may still be practical for smaller telescopes such as the HabEx concept, large telescopes where even average-sized stars represent significant tip/tilts likely require additional pupil apodization or different focal plane masks to sufficiently control diffraction from their struts and segment gaps. We intend to investigate in a future paper whether using DMs with more actuators or using a smaller aperture telescope/imaging smaller stars improves performance sufficiently for 1D-optimized DM-augmented coronagraphs to be viable.

ACKNOWLEDGMENTS

This work was performed at the Jet Propulsion Laboratory, California Institute of Technology, under a contract with the National Aeronautics and Space Administration. This work was supported by an appointment to the NASA Postdoctoral Program at the Jet Propulsion Laboratory, administered by the Universities Space Research Association under contract with NASA.

REFERENCES

[1] Noecker, M. C., Zhao, F., Demers, R., Trauger, J., Guyon, O., and Kasdin, J. N., "Coronagraph Instrument for WFIRST-AFTA", JATIS, 2, 011001 (2016)

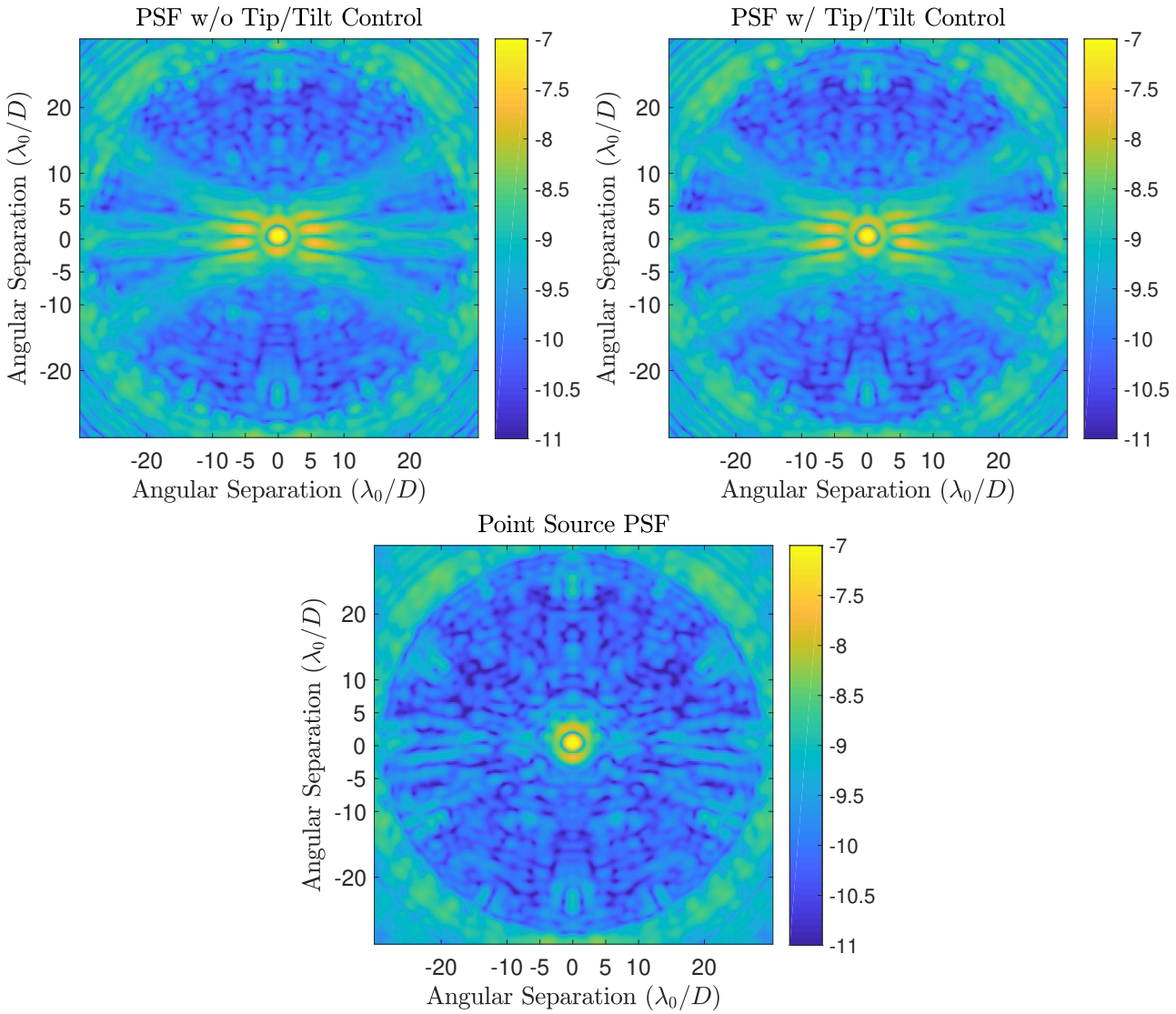

Figure 6. Point-spread functions for our DMSPLC using a 1 mas diameter star without tip/tilt control, with tip/tilt control, and using a point source instead. The DMs are not able to fully correct the diffraction from the struts, segment gaps, and finite-sized star simultaneously, resulting in a factor of $\sim 4-5$ degradation in contrast at an inter-DM Fresnel number of 576.

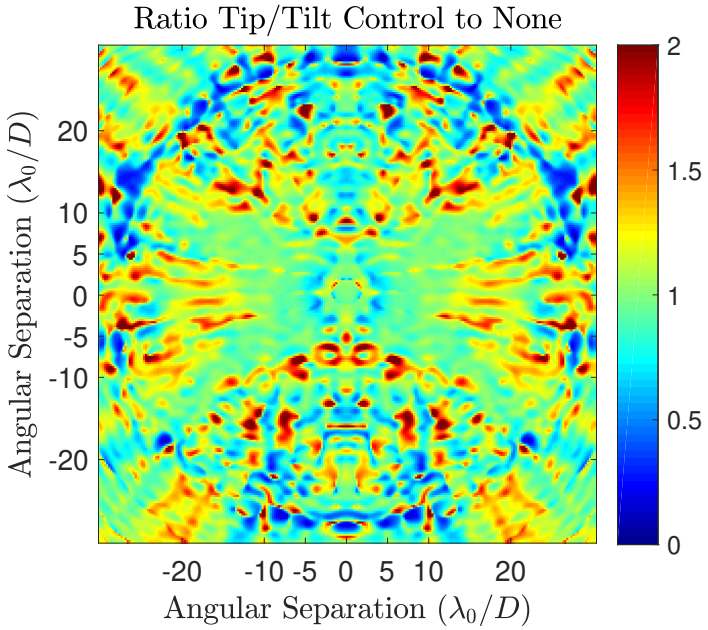

Figure 7. Ratio of the intensity in the dark hole for a 1 mas star with tip/tilt control enable vs. without (the top left and top right panels of Figure 6). Overall, enabling tip/tilt control did not result in better light control within the dark hole; instead, light was largely merely moved around. The main corrective benefit occurred at the maximum correction radius, which is significantly darker with tip/tilt control enabled.

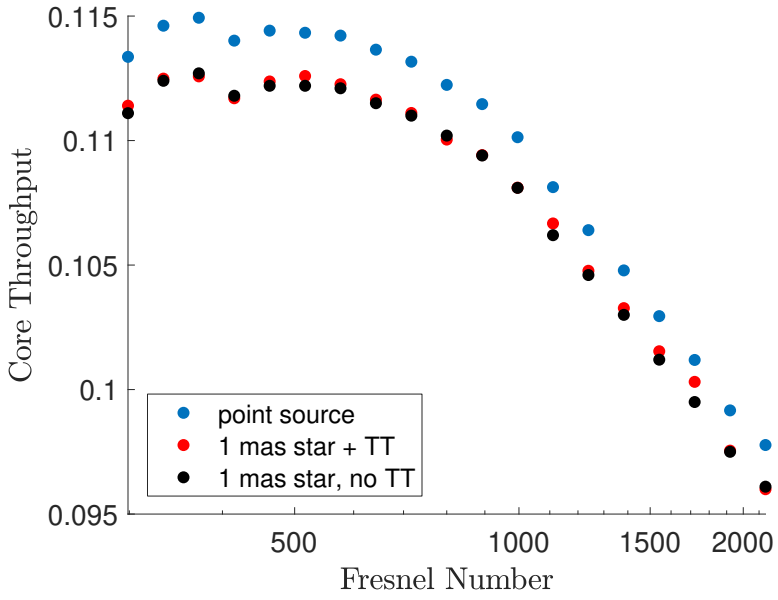

Figure 8. Throughput as a function of Fresnel number for our 2D FALCO simulations. The parameters for each point are identical to those in Figure 5. The throughput decreases only a small amount when a 1 mas diameter star is used instead of a point source.

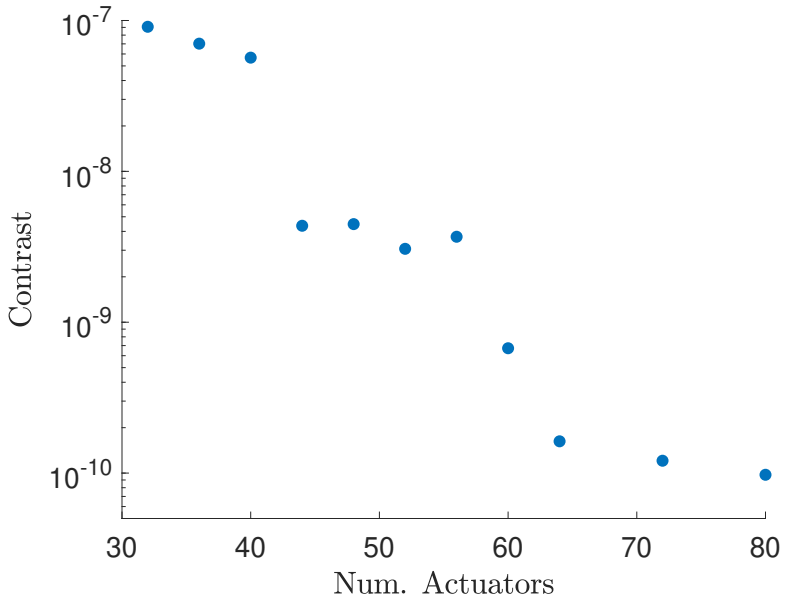

Figure 9. Contrast vs. number of actuators across the DM for our 2D FALCO simulations, using a point source star at an inter-DM Fresnel number of 576.1. We do not have a definitive explanation for stairstep behavior seen in the Figure. 64x64 DMs are sufficient to reach 10^{-10} contrast, with larger ones appearing to provide little benefit for the size of our dark hole.

[2] Bolcar, M. R., Aloezos, S., Bly, V. T., Collins, C., Crooke, J., Dressing, C. D., Fantano, L., Feinberg, L. D., France, K., Gochar, G., Gong, Q., Hylan, J. E., Jones, A., Linares, I., Postman, M., Pueyo, L., Roberge, A., Sacks, L., Tompkins, S., and West, G., "The Large UV/Optical/Infrared Surveyor (LUVOIR): Decadal Mission concept design update", Proc. SPIE, 10398, 1039809 (2017)

[3] Mennesson, B., Gaudi, S., Seager, S., Cahoy, K., Domagal-Goldman, S., Feinberg, L., Guyon, O., Kasdin, J., Marois, C., Mawet, D., Tamura, M., Mouillet, D., Prusti, T., Quirrenbach, A., Robinson, T., Rogers, L., Scowen, P., Somerville, R., Stapelfeldt, K., Stern, D., Still, M., Turnbull, M., Booth, J., Kiessling, A., Kuan, G., and Warfield, K., "The Habitable Exoplanet (HabEx) Imaging Mission: preliminary science drivers and technical requirements", Proc. SPIE, 9904, 99040L (2016)

[4] Davies, R., Schubert, J., Hartl, M., et al., "MICADO: first light imager for the E-ELT", Proc. SPIE, 9908, 99081Z (2016)

[5] Brandl, B. R., Agócs, T., Aitink-Kroes, G., et al., "Status of the mid-infrared E-ELT imager and spectrograph METIS", Proc. SPIE, 9908, 990820 (2016)

[6] Larkin, J. E., Moore, A. M., Wright, S. A., Wincentsen, J. E., Anderson, D., Chisholm, E. M., Dekany, R. G., Dunn, J. S., Ellerbroek, B. L., Hayano, Y., Phillips, A. C., Simard, L., Smith, R., Suzuki, R., Weber, R. W., Weiss, J. L., and Zhang, K., "The Infrared Imaging Spectrograph (IRIS) for TMT: instrument overview", Proc. SPIE, 9908, 99081W (2016)

[7] Riggs, A., Ruane, G., Sidick, E., Coker, C., and Kern, B. D., "Fast linearized coronagraph optimizer (FALCO) I: a software toolbox for rapid coronagraphic design and wavefront correction", Proc. SPIE, 10698-101 (2018)

[8] Sidick, E., Riggs, A., Ruane, G., Krist, J., Moody, D., and Coker, C., "Fast Linearized Coronagraph Optimizer (FALCO) II: Optical Model Validation and Time Savings over Other Methods", Proc. SPIE, 10698-165 (2018)

[9] Mazoyer, J., Pueyo, L., N'Diaye, M., Goarty, K., Zimmerman, N., Leboulleux, L., St. Laurent, K. E., Soummer, R., Shaklan, S., and Norman, C., "Active Correction of Aperture Discontinuities-Optimized Stroke Minimization. I. A New Adaptive Interaction MAtrix Algorithm", AJ, 155, 7 (2018)

[10] Diamond, S., and Boyd, S., "CVXPY: A Python-Embedded Modeling Language for Convex Optimization", Journal of Machine Learning Research, 17, 83 (2016)

[11] Agrawal, A., Verschueren, R., Diamond, S., and Boyd, S., "A Rewriting System for Convex Optimization Problems", Journal of Control and Decision, 5, 1 (2018)

[12] Stark, C. C., Roberge, A., Mandell, A., and Robinson, T. D., "Maximizing the ExoEarth Candidate Yield from a Future Direct Imaging Mission", ApJ, 795, 122 (2014)

[13] Poyneer, L. A., Bauman, B., Cornelissen, S., Isaacs, J., Jones, S., Macintosh, B. A., and Palmer, D. W., "The use of a high-order MEMS deformable mirror in the Gemini Planet Imager", Proc. SPIE, 7931, 793104 (2011)

[14] Mazoyer, J., Pueyo, L., N'Diaye, M., Fogarty, K., Zimmerman, N., Soummer, R., Shaklan, S., and Norman, C., "Active Correction of Aperture Discontinuities-Optimized Stroke Minimization. II. Optimization for Future Missions", ApJ, 155, 8 (2018)